The evolution of octahedral rotations of orthorhombic $LaVO_3$ in superlattices with cubic $SrVO_3$

U. Lüders* and Q.-R. Li

CRISMAT, UMR CNRS ENSICAEN 6508;

6 boulevard Maréchal Juin, 14050 Caen cedex 4, France

R. Feyerherm and E. Dudzik

Helmholtz-Zentrum Berlin für Materialien und Energie GmbH, BESSY;

12489 Berlin, Germany

(Dated: June 26, 2014)

Abstract

We have studied the octahedral rotations in $LaVO_3/SrVO_3$ superlattices, keeping the thickness of the orthorhombic $LaVO_3$ layers constant and increasing the thickness of cubic $SrVO_3$ layers. We have found that for a small thickness of $SrVO_3$, the octahedral rotations in $LaVO_3$ are maintained, while for an increasing thickness, these rotations are suppressed. This observation cannot be explained by purely elastic effects due to the lattice mismatch between the two materials, but the absence of rotations in $SrVO_3$ is a crucial ingredient, illustrating the concept of interface engineering of octahedral rotations.

PACS numbers: 68.65.Cd, 61.05.cp, 68.55.jm

*Electronic address: ulrike.luders@ensicaen.fr

I. INTRODUCTION:

The structure of the cubic perovskite oxides ABO_3 can be described by a corner-sharing network of BO_6 octahedra, with the B ion in its center, the A ion is positioned on a dodecahedral site in the middle of the cube. However, in many perovskite oxides, these octahedra are tilted around its center, transforming the basic cubic structure into a lower-symmetry structure, as for example the orthorhombic or monoclinic one [1], depending on the details of the octahedral rotations. These rotations of the oxygen octahedra have been shown to play a major role in different specific properties of this group, as for example ferroelectricity [2–4], the magnetic structure [5–7] and the resistive behavior [6]. This is due to the fact that the octahedral rotations influence the B-O bond length and B-O-B angle due to the shift of the oxygen ions from the edges of the cubic perovskite structure. On the other hand, both the B-O bond length and the B-O-B angle play a major role for the determination of the bandwidth [8] and the magnetic interactions [9, 10]. The introduction or modification of octahedral rotations would therefore constitute an important tool to tune the properties of perovskite oxides.

Octahedral rotations manifests typically in the case that the A ion is too small for the cubic BO_6 corner-sharing network [1], but they are also an important degree of freedom for the accommodation of pressure or strain in the perovskite structure. It is even one of the most efficient mechanisms to distort the structure under applied pressure, especially in systems in which other electronically induced effects such as the Jahn-Teller-effect are weak. Epitaxial strain generated by the lattice mismatch at heterointerfaces in thin films was observed to be accommodated by the change of the octahedral rotations in several perovskite systems [5, 11–15]. Most of these heterointerfaces do not only imply a mismatch because of the difference of the lattice parameter, but also the tilt system of the oxygen octahedra may change from one oxide to the other. The collective character of these rotations due to the corner-shared octahedral network reaching across the perovskite-perovskite interface may result in the introduction or reduction of rotations in the vicinity of these interfaces, especially in the case of a strong difference of the tilt angle at the interface. Thus, a tilt system mismatch may also be used to induce changes in the octahedral rotations of the involved materials.

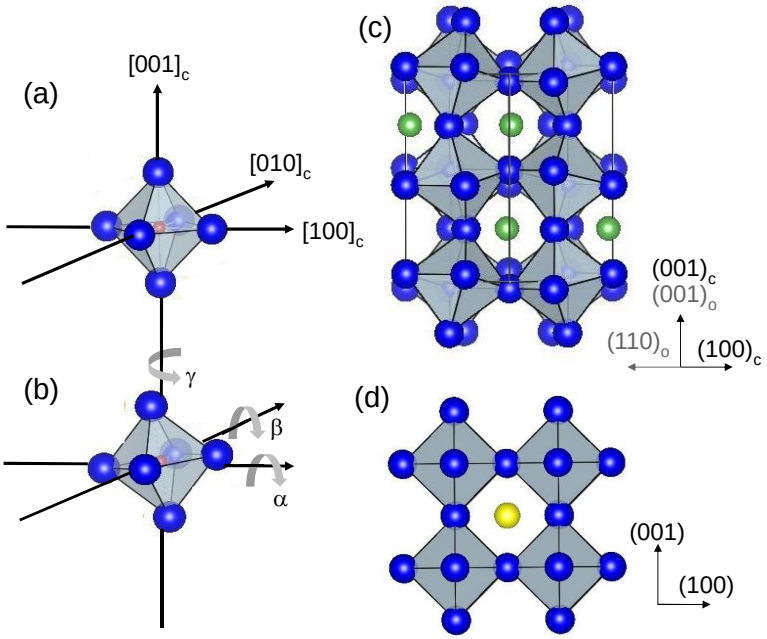

FIG. 1: (color online) (a) VO_6 octahedron with the cubic reference axis and (b) rotated octahedron in the same reference system. Representation of the orthorhombic unit cell of bulk $LaVO_3$ (blue: O, green: La, red: V) (c), and the cubic unit cell of bulk $SrVO_3$ (yellow: Sr) (d).

One of the most widely-used notations to describe a tilt system is the Glazer notation [16]. It relies on the description of the rotation of the octahedra in a pseudo-cubic reference structure. This reference structure corresponds to the cubic perovskite structure without rotations, where the equatorial plane of the octahedron lies in the (001) plane, and the apical oxygen atoms are aligned along the [001] direction (see Figure 1 (a)). A possible rotation of the octahedron is firstly described by the amplitude of the rotation around each of the three axes. This can be done either by the tilt angle of the octahedron α, β and γ around each of the three reference axis (see Figure 1 (b)), or, as in the Glazer system, by the lattice parameter of the pseudo-cubic unit cell a_p, b_p and c_p. It was shown that these lattice parameters are directly related to the tilt angles [16], so that the relative amplitude of the rotations around each axis are described by three letters, where the equality of two letters indicate the same tilt angles around the corresponding axes. Furthermore, the relative rotation direction from one octahedron to the other along each axis has to be integrated

into the description in order to account for the symmetry of the resulting structure. There are two possibilities: either the neighbouring octahedron rotates in the same direction (in-phase rotation), or the octahedron turns in the opposite direction (antiphase rotation). In the first case, the in-phase rotation is noted as a + superscript of the corresponding axis. For antiphase rotations, a - superscript is used. The superscript 0 indicates that there is no rotation around the corresponding axis. This notation has two advantages: first, the notation allows to describe in a condensed way the characteristics of a tilt system, and second, the comparison of different tilt systems is easy.

The change in the tilt systems at heterointerfaces is not widely studied experimentally, principally because of technically demanding experiments. Depending on the involved materials, the modifications of the octahedral rotations can be observed throughout a thin film and therefore in macroscopic measurements [13], or only in a few monolayers at the interface [5]. In the latter case, local techniques with a high spatial resolution have to be employed. A way to avoid local techniques is the study of superlattices, where two materials with a thickness of only a few monolayers are periodically repeated, leading to a high number of interfaces. Macroscopic techniques as X-ray diffraction can be used in this case to study the octahedral rotations. A second advantage of the superlattices is that the thickness of each material can be changed independently, allowing to study the stabilization of the tilt system depending on the thickness of each material. This was done in the system $LaNiO_3/SrMnO_3$ [15], forming a heterointerface between a material with an ($a^-a^-a^-$) tilt system in the Glazer notation and a cubic perovskite without rotations ($a^0a^0a^0$). The collective character of the rotations through the interface was shown by the disappearance of the rotations below a critical thickness of $LaNiO_3$.

In this work, we will report on a similar study of the octahedral rotations in $LaVO_3/SrVO_3$ superlattices. Bulk $LaVO_3$ at room temperature is an orthorhombic perovskite, adopting the *Pnma* structure [17] with the corresponding ($a^-b^+a^-$) tilt system [1, 16]. Figure 1 (c) shows the orthorhombic unit cell and the corresponding pseudocubic description. The antiphase rotations along the $[100]_c$ and the $[001]_c$ axis and the resulting displacements of the oxygen atoms are clearly visible in this view. Bulk $SrVO_3$ on the other hand, is a cubic perovskite (see Figure 1 (d)) without octahedral rotations, and thus the tilt system ($a^0a^0a^0$) [18]. Figure 1 (c) and (d) show these structures projected on the (010) plane, where the [001] direction corresponds to the growth direction. In the case of the intergrowth of these two materials in

a superlattice on a (001) oriented substrate, interfaces corresponding to the Figure 1 (c) and (d) will be created. The metrical mismatch can be calculated to be 2% on the basis of the bulk pseudocubic lattice parameters of 3.925 Å for $LaVO_3$ and 3.843Å for $SrVO_3$. However, $LaVO_3$ is known to grow coherently strained on $SrTiO_3$ substrates [11] with an in-plane lattice parameter near to 3.905Å, so the actual mismatch in the superlattice is even smaller. In addition to the difference of the in-plane lattice parameters, the oxygen atoms at the interface will have to adopt a different equilibrium position than in the corresponding bulk materials, as they are shared between the two structures. The adaptation of a structure with octahedral rotations to a structure without octahedral rotations can be realized in two ways: if the bulk rotational patterns of each material are kept at the interface, the octahedra will be distorted in order to accommodate the different equilibrium positions of the oxygen atoms. If the octahedra are hard to distort, the change of the tilt system at the interface will be gradual, leading therefore either to induced octahedral rotations in the formerly untilted cubic material, or to the suppression of the octahedral rotations in the orthorhombic material.

The aim of this work is to study which of these two situations is realized in the superlattices of $LaVO_3$ and $SrVO_3$. Accordingly, superlattices were studied, where the thickness of the cubic material was varied. It was already shown that in thin films of $LaVO_3$ on $SrTiO_3$ under compressive strain, a bulk-like tilt system [11] is conserved where only the amplitudes of rotation are modified resulting in an ($a^-a^+c^-$) tilt system. By the intergrowth with different thickness of $SrVO_3$, it will be possible to study the evolution of the tilt system adapted by the superlattice when the $LaVO_3$ tilt system is perturbed.

II. EXPERIMENTAL

The samples were prepared by Pulsed Laser Deposition on $SrTiO_3$ (001) substrates, details are described elsewhere [19]. The thickness of the $LaVO_3$ layer was kept constant at 6 unit cells, while the thickness of the $SrVO_3$ layer was varied between 1 and 6 unit cells. The notation of a $(LaVO_3)_6/(SrVO_3)_n$ superlattice throughout this paper will be $6/n$, the first (second) number indicating the thickness in unit cells of $LaVO_3$ ($SrVO_3$). The calibration of the growth rate by test superlattices for the individual materials constituting the superlattice was confirmed by the analysis of the superlattice satellites observed in the X-

ray Diffraction measurements (XRD). The number of repetitions of the bilayer was adjusted so that the total thickness of all superlattices was close to 80nm. XRD measurements of the Bragg peaks were carried out with a Seifert diffractometer as well as a high-precision diffractometer using a 18kW rotating anode generator, both using Cu $K_{\alpha 1}$ (λ = 1.5405 Å) wavelength. Superstructure reflexions were studied using the four circle diffractometer at beamline 7T-MPW-MAGS at the synchrotron source BESSY II at Helmholtz-Zentrum, Berlin. A photon energy of 12.398 keV was chosen (λ = 1 Å).

Throughout this article, we will use the pseudo-cubic description of the $LaVO_3$ structure and the corresponding indexation of the reflections, as the Glazer description of the tilt systems relies on the pseudo-cubic unit cell [16]. The relation of this description with respect to the more correct orthorhombic description of the system is shown by H. Rotella *et al.* [11]. We did not find any indication that the two in-plane parameters a_p and b_p are different within the precision of the measurements as expected by the use of a cubic substrate; we shall therefore set $a_p = b_p$. a_p and the out-of-plane lattice parameter c_p are calculated on the basis of orthogonal axes, although a small inclination of the c-axis with respect to the $(a - b)$ plane cannot be excluded. However, if present, this inclination is small enough not to alter the main observations of the presented results.

The measured intensity of half-order reflections related to the rotations was normalized to enable the comparison of the same reflections of different samples. The measured intensity is divided by the ring current in order to correct fluctuations of the incoming light intensity, and by the maximum intensity of the corresponding full-order substrate peak to correct any small misalignments of the sample.

The resistivity measurements were carried out with four Ag contacts on the superlattice surface. The depth of the electrical contact into the superlattice is estimated to be around 10nm due to the use of ultrasonic wire bonding. The measurements were carried out in a Physical Properties Measurement System by QuantumDesign. The resistivity of the superlattices was calculated by taking into account the full thickness of the superlattice.

III. RESULTS

The structural properties of the superlattices used in this study are shown in Fig. 2 (a). The observed reflections of the superlattice can be indexed in the pseudocubic repre-

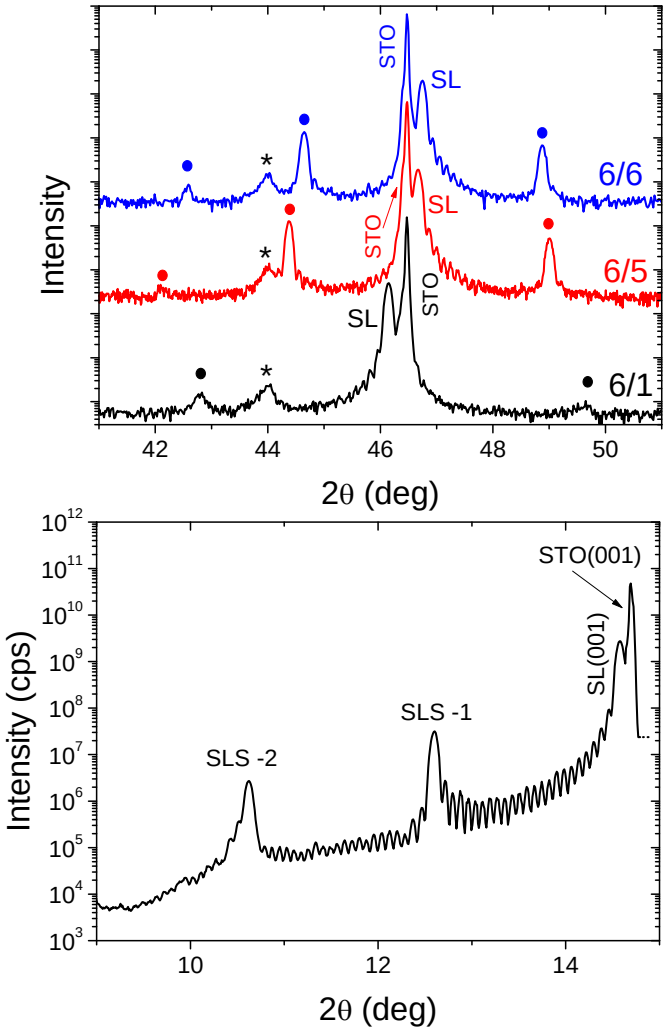

FIG. 2: (color online) (a) $\theta - 2\theta$ XRD pattern around the (002) reflection of 6/1 (black), 6/5 (red) and 6/6 (blue) superlattice. Superlattice Bragg peaks are marked by SL, substrate Bragg peaks by STO. Superlattice satellites are marked by a filled circle, the peak indicated by a star is due to the sample holder. (b) $\theta - 2\theta$ XRD pattern of the 6/1 superlattice at the low angle side of the (001) Bragg peak. Superlattice satellites are marked by SLS and their order.

sentations being $(00l)$ reflections, so the out-of-plane direction corresponds to that of the substrate. Laue fringes and superlattice satellites (marked by a filled circle) are observed in the vicinity of the superlattice Bragg peaks, indicating a high structural coherence of the film and the layered character of the superlattices. Notably, the superlattice with only one unit cell of $SrVO_3$ shows distinct superlattice satellites (see Fig. 2 (b)), so even for such a low $SrVO_3$ thickness, the additional periodicity of the superlattice due to its layered

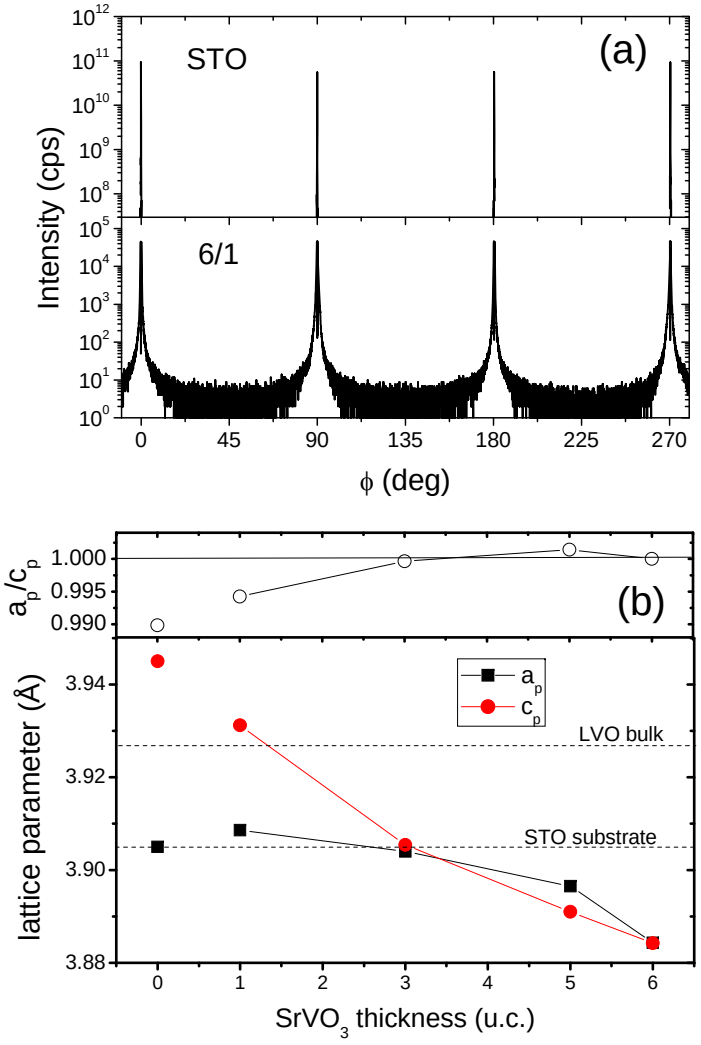

FIG. 3: (color online) (a) *phi*-scan of the (103) reflection of the $SrTiO_3$ substrate (top panel) and a 6/1 superlattice (bottom panel) showing a cube-on-cube epitaxy. (b) Bottom panel: in-plane a_p and out-of-plane c_p lattice parameters of the superlattices *vs* the thickness of the $SrVO_3$ layer. A thickness of 0 u.c. of $SrVO_3$ indicates the lattice parameters of a $LaVO_3$ thin film (taken from [11]). The dashed lines indicate the $LaVO_3$ bulk pseudo-cubic and the $SrTiO_3$ bulk lattice parameters. Top panel: ratio a_p/c_p, a ratio of 1 is indicated by the line.

character is confirmed, excluding the formation of a solid solution as a result of a possible intermixing or interdiffusion.

The superlattices grow epitaxially on the substrate, with a cube-on-cube orientation as

observed already in other studies [19–21]. In Fig. 3 (a), a phi-scan of the (103) reflection of a 6/1 superlattice and of the substrate illustrates this epitaxial relationship by the coincidence of the peak positions with respect to ϕ. a_p and c_p are calculated with the position of the observed (00l) and the mean position of the <103> reflection family. Line scans were used for this purpose, but the comparison with reciprocal space maps of some of the reflections verified the reliability of the optimization procedure of the line scans. As can be also observed in Fig. 2 (a), both a_p and c_p diminish with increasing $SrVO_3$ thickness (Fig. 3(b)). For the sake of comparison, the lattice parameters observed in a thick $LaVO_3$ film on $SrTiO_3$ [11] are included, as well as the ratio a_p/c_p for all samples. For a small thickness of $SrVO_3$, a_p/c_p of the superlattice takes a value smaller than 1, somewhat different from the value observed in the thick film, but the strain state indicated by the value of a_p similar to that of the substrate is comparable. Above a thickness of 3 monolayers of $SrVO_3$, a_p/c_p approaches one, with the lattice parameters diminishing from a value comparable to the STO value to smaller ones, although the lattice parameter of bulk $SrVO_3$ (3.843 Å [22]) is far from being reached.

Concerning the tilt system of the oxygen octahedra, we have observed certain half-order reflections generated by the additional periodicity of the tilt system. The ($a^-a^+c^-$) tilt system, observed in the $LaVO_3$ thick film, is characterized by one in-plane axis with in-phase rotations. The first step to analyze the tilt system of the superlattices is therefore to determine the presence and the direction of this axis. In-phase rotations produce (integer half-integer half-integer), (half-integer integer half-integer) or (half-integer half-integer integer) reflections [16], depending on the orientation of the in-phase axis in the sample. We have chosen the family of $<1\ \frac{3}{2}\ \frac{1}{2}>$ because of their relatively strong intensity. The measurements of this family are shown in Fig. 4 for superlattices with different $SrVO_3$ thickness. The 6/1 superlattice shows a finite intensity of the $(1\ \frac{3}{2}\ \frac{1}{2})$ and the $(\frac{3}{2}\ 1\ \frac{1}{2})$ reflection, while the $(\frac{3}{2}\ \frac{1}{2}\ 1)$ reflection is absent. Thus, the axes carrying in-phase rotations are lying in-plane, the out-of-plane axis does not carry in-phase rotations.

The observation of the two in-plane axes carrying in-phase rotations differs on a first sight from the tilt system observed in $LaVO_3$ bulk or thin films. However, it was shown that the orthorhombic structure of $LaVO_3$ in superlattices shows two in-plane structural variants [20], which are 90° apart. These variants occur because of the particular orientation of the orthorhombic $LaVO_3$ unit cell during the growth on (001)-oriented cubic substrates: one

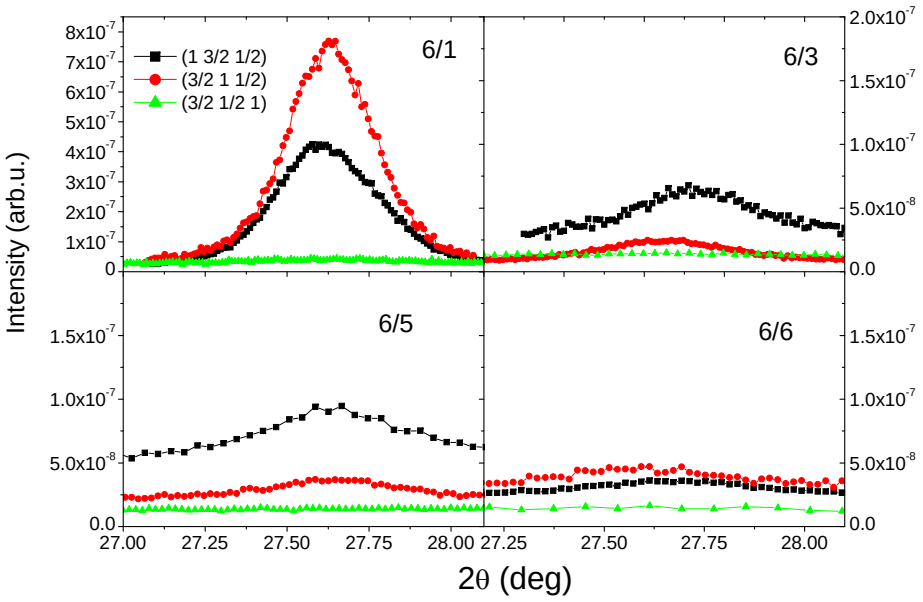

FIG. 4: (color online) θ-2θ patterns of half-order reflections produced by in-phase octahedral rotations for a 6/1 (top left), 6/3 (top right), 6/5 (bottom left) and 6/6 (bottom right) superlattice.

of the axes carrying antiphase rotations is oriented in-plane, resulting in a doubling of the unit cell in this direction with respect to the pseudo-cubic one and therefore to a structural anisotropy in the plane. $SrTiO_3$ being cubic, the long axis of the $LaVO_3$ orthorhombic unit cell can be oriented along each of the two perpendicular in-plane directions, leading to two different in-plane orientations of the film. Therefore, regarding the tilt system of the superlattice, the intensity of the half-order reflections in both in-plane directions may be only a result of the two variants, each comprising an in-plane axis with in-phase rotations and one with antiphase rotation as in the bulk tilt system.

This hypothesis can be confirmed by the observation of the $(\frac{1}{2}\ \frac{1}{2}\ \frac{5}{2})$ reflection, which is related only to antiphase rotations in the plane of the film [16]. In the case that both of the two in-plane directions carry only in-phase rotations, this reflection should be extincted. Fig. 5 (a) shows the presence of this reflection for the 6/1 superlattice, so an axis carrying antiphase rotations is present in the plane of the film. Combining the results on the in-phase and antiphase rotations, the tilt system of each variant of the superlattice is constituted by one in-plane axis carrying in-phase rotations and one carrying antiphase rotations, as in the bulk tilt system.

The amplitude of the octahedral rotations can be estimated from the lattice parameters

of the film [16]. The observation of the in-plane variants indicates that the two pseudo-cubic in-plane lattice parameters a_p and b_p are equal, and we do not have any further evidence that a_p and b_p of the superlattices could be different, for example by the relative positions of the <103> family. The equality of a_p and b_p is also the expected case, as the substrate is cubic. This fact results thus in equal amplitudes (or rotation angles) for the two in-plane directions of the superlattice. c_p was shown to be different from a_p in the 6/1 superlattice (Fig. 3 (b)), so the amplitude of the antiphase rotations around the (001) direction is different from the one in plane. Summarizing this discussion of the tilt system in the 6/1 superlattice, it can be described as ($a^-a^+c^-$), as the one observed in $LaVO_3$ thin films. Unfortunately, we were not able to measure enough independent reflections of the tilt system (and which do not show any contribution on the intensity due to a displacement of La) to determine unequivocally the values of the rotation angles.

The chosen technique for the characterization of the tilt system, XRD, is a macroscopic technique, so that the tilt system of the whole superlattice is characterized, and a distinction between the two constituent materials is not possible. However, only one of the materials, $LaVO_3$, shows octahedral rotations in bulk [17] and in thin films [11], with the same tilt system observed in the 6/1 superlattice. So the tilt system of the superlattice seems to be governed by the rotations present in $LaVO_3$ thin films, which is not surprising given the very low thickness of the $SrVO_3$ layers. The main observation so far is thus that the introduction of a single unit cell of $SrVO_3$ appears not to alter drastically the octahedral rotations of the $LaVO_3$.

Increasing the thickness of the $SrVO_3$ layer in the superlattice, the intensity of the half-order reflections decreases strongly. Please note, that in Fig. 4, the intensity scale for the 6/3, 6/5 and 6/6 superlattices is four times smaller than the one for the 6/1 superlattice. This decreasing intensity, which is observed for all analyzed half-order reflections (Fig. 5), indicates that the rotation angle decreases strongly with increasing $SrVO_3$ thickness [15, 16]. While in the 6/3 and 6/5 superlattices, a small intensity is still observable, the 6/6 superlattice shows nearly no intensity of the half-order reflections anymore.

This decrease of the half-order reflections related to the tilt system of $LaVO_3$ could be a result of the diminishing volume of $LaVO_3$ in the superlattice. The samples were prepared with a constant total thickness, so the increase of the $SrVO_3$ thickness is related to a decrease of the $LaVO_3$ volume fraction in the superlattice. If the decrease of the intensity would be

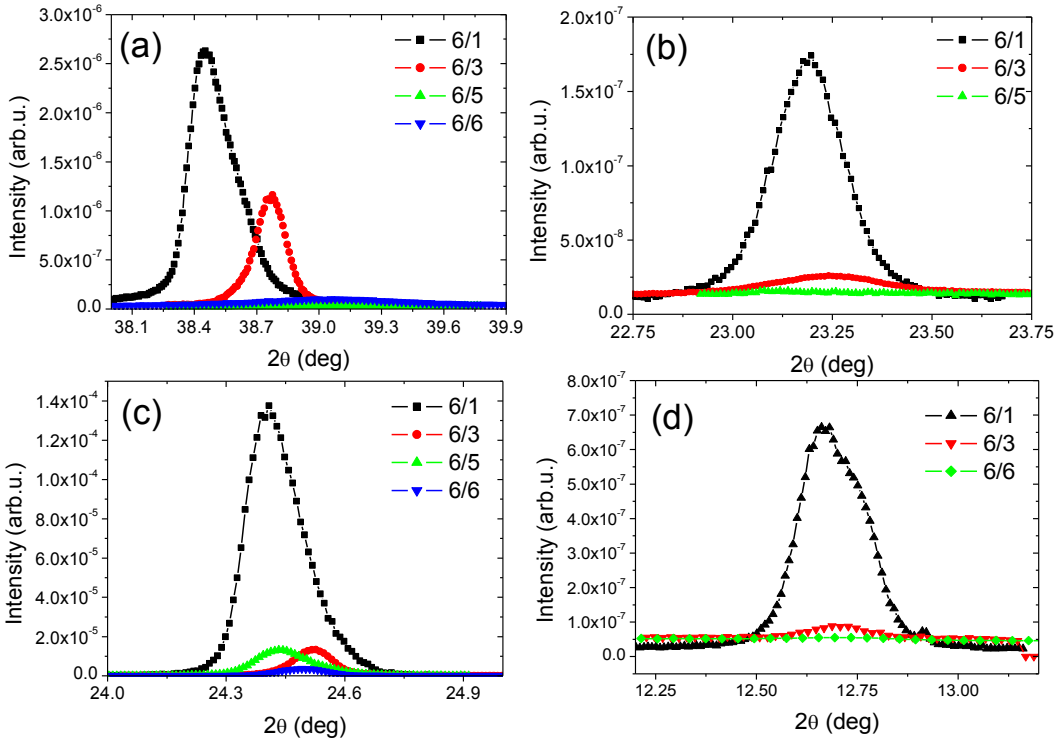

FIG. 5: (color online) θ-2θ pattern of the $(\frac{1}{2}\ \frac{1}{2}\ \frac{5}{2})$ reflection (a), the $(\frac{1}{2}\ 0\ \frac{3}{2})$ reflection (b), the $(\frac{1}{2}\ \frac{3}{2}\ \frac{1}{2})$ reflection (c) and the $(\frac{1}{2}\ \frac{1}{2}\ \frac{1}{2})$ reflection (d) for different superlattices.

solely related to the smaller volume of the $LaVO_3$ layers, the intensity should decrease by roughly a factor of 2 going from the 6/1 superlattice to the 6/6 one, and not by the observed factor of 16. Another possibility would be a change of the tilt system, the resulting one extincting the observed half-order reflections. However, the presented half-order peaks probe all possible in-phase or antiphase rotations in the three directions: the absence of intensity of the $(1\ \frac{3}{2}\ \frac{1}{2})$, $(\frac{3}{2}\ 1\ \frac{1}{2})$, $(\frac{3}{2}\ \frac{1}{2}\ 1)$ (Fig. 4) and $(\frac{1}{2}\ 0\ \frac{3}{2})$ (Fig. 5 (b)) indicate the absence of in-phase rotations in all three directions. The absence of intensity of the $(\frac{1}{2}\ \frac{1}{2}\ \frac{5}{2})$ (Fig. 5 (a)) excludes antiphase rotations around the (100) and the (010) direction, and the absence of $(\frac{1}{2}\ \frac{3}{2}\ \frac{1}{2})$ (Fig. 5 (c)) antiphase rotations around the (100) and the (001) direction. Therefore, the only possible tilt system is $(a^0a^0c^0)$, i.e. the absence of octahedral rotations in the superlattice. Thus, the introduction of thick layers of a material without octahedral rotations ($SrVO_3$) reduces the rotations also in the neighboring material prone to them.

Apart from the half-order reflections directly related to the octahedral rotations, the $(\frac{1}{2}$

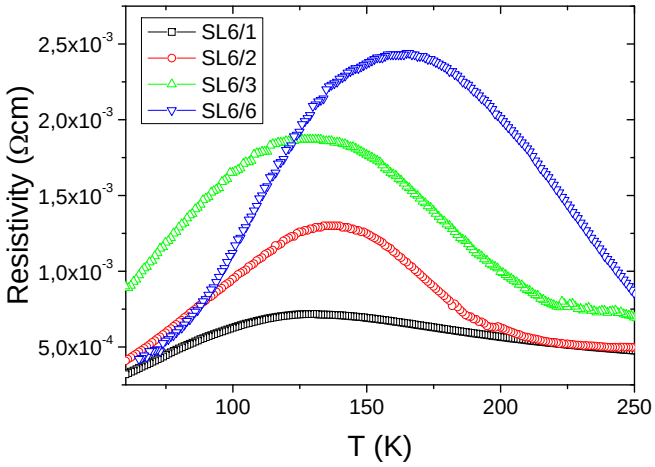

FIG. 6: (color online) Resistivity *vs* temperature of superlattices with different $SrVO_3$ thickness

$\frac{1}{2}$ $\frac{1}{2}$) reflection was also observed. It shows still a finite intensity for the 6/1 superlattice, which diminishes again strongly with increasing thickness of $SrVO_3$ (see Fig. 5 (d)). As this reflection is related to the orthorhombic symmetry of the unit cell [11, 17], the disappearance for superlattices with thick $SrVO_3$ layers illustrate well the change in symmetry of the unit cell to a (not only metrically) cubic one.

As discussed in the introduction, the modification of the octahedral transitions may have a strong influence on the magnetic or resistive properties of the material. In order to elucidate the effect of the observed suppression of the octahedral rotations on the properties of the superlattices, their in-plane resistivity was measured (Figure 6). The overall temperature dependence of the resistivity is the same for all superlattices: a low resistivity, metallic state at low temperature, with a transition to a state of higher resistivity at a temperature of around 150K. The suppression of the octahedral rotations does not alter this general behavior, although an enhancement of the maximum resistivity with the thickness of $SrVO_3$ can be observed. The resistivity maximum itself was discussed in detail for the 6/1 superlattice [21], where the resistive transition was related to the structural transition of $LaVO_3$. The maximum of the resistivity can be used therefore as a probe of the structural transition of the $LaVO_3$ layers in the superlattice. It can be observed that the temperature of the resistivity maximum increases with the thickness of the $SrVO_3$ layer, a detailed discussion of this observation will be done in the following section.

IV. DISCUSSION

We observe the suppression of the octahedral rotations in an orthorhombic oxide, $LaVO_3$, at the interface with an oxide without octahedral rotations, $SrVO_3$. The thickness of 6 unit cells of the $LaVO_3$ layer may be close to the maximum thickness to have the $SrVO_3$ suppress the rotations completely throughout the whole $LaVO_3$ layer, as it was shown that the alteration of the rotations at the interface between two materials reaches up to 4 monolayers into the materials [5, 12]. These findings shed a new light on some systems with interesting properties originating at the interface between materials with and without octahedral rotations, as for example $SrTiO_3/LaAlO_3$ [23]. The fact that at perovskite oxide interfaces, the octahedral network reaches through the interface, forces the materials to accommodate not only the lattice mismatch, but also the 'rotational mismatch'. The only way to change abruptly from one rotational pattern to the other is to distort the equatorial plane of the octahedra, which in most $A^{3+}B^{3+}O_3$ perovskites is energetically extremely unfavorable. It is much more favorable to alter the rotational pattern, as this distorts the A ion cuboctahedra, which then in turn leads to the modification of the octahedral rotations at both sides of the interface. These observations are in agreement with other studies of the octahedral rotations in systems with one material exhibiting octahedral rotations combined with another material without them [15], where also a modification of the rotational pattern is observed rather than the distortion of the octahedra.

However, the modification of the octahedral rotations are also an important way of lattice accommodation. $SrVO_3$ has a smaller pseudo-cubic lattice parameter than $LaVO_3$. When the number of $SrVO_3$ layers in $LaVO_3/SrVO_3$ superlattices increases, the mean pseudo-cubic lattice parameter decreases, as shown in Figure 3(b), and so does the mean unit cell volume. When deposited on $SrTiO_3$, the mean stress state of the superlattice is therefore compressive for $n<2$ and tensile for $n > 2$. As the lattice parameters reported in Fig. 3 have been measured by X-ray diffraction, they represent the value averaged over the entire superlattice rather than the individual sets of lattice parameters from each constituent of the superlattice. It is therefore on these mean values that the following analysis is based. The compressive stress exerted by the substrate on the superlattices with a thin $SrVO_3$ layer imposes an in-plane lattice parameter of the superlattice smaller than the bulk one of $LaVO_3$, and consequently an out-of-plane mean lattice parameter larger than the mean

pseudo-cubic one. For less than two layers of $SrVO_3$, the superlattice exhibits therefore a tetragonal distortion of the pseudo-cubic unit cell with $a_p/c_p < 1$. As the stress state switches from compressive to tensile (i.e. for n≥2) c_p of the superlattice decreases until becoming equal to a_p and keeps on decreasing as the thickness of the $SrVO_3$ layers increases. a_p decreases, too, and becomes different from the substrate's lattice parameter, indicating that dislocations are created in order to accommodate for the mismatch growing with the number of $SrVO_3$ layers.

The purely elastic picture, in which only the metrical mismatch is taken into account, explains the trend of the lattice parameters of the superlattice when the $SrVO_3$ thickness increases. However, a stronger decrease of c_p as observed would be expected in this picture, which is based on a constant unit cell volume, as the influence of oxygen octahedral rotations are omitted. Under tensile strain, it has been shown [14] that the octahedral rotations around the c-axis tend to be reduced. This can be understood in the simple picture that in the case of octahedral rotations, the oxygen atoms are displaced from the edge of the cube, approaching the atoms in the unit cell without decreasing the bond length. In the case of tensile strain, the opposite effect holds: the lattice parameter is increased without enhancing the bond lengths by the reduction of the octahedral rotations around the (001) direction. The suppression of the octahedral rotations around the out-of-plane direction in the superlattices can therefore be understood on the basis of the tensile strain exerted by the substrate, leading to the elastic decrease of c_p. But also the rotations around the in-plane directions have to be taken into account. The observed suppression of these rotations in the superlattices enlarges both a_p and c_p. So again, the accommodation of the tensile strain in the plane of the superlattice leads to the suppression of the rotations, but in this case, c_p is enlarged, too, leading to a partial compensation of the elastic decrease of c_p.

The disappearance of in-plane tilts under tensile strain may appear in contradiction with earlier reports of thin films on various substrates [14] or calculations under various strain states [24], where it was observed that the rotations around the in-plane axes are not suppressed. This contradiction is only apparent as in these studies, *strain* was imposed on the *same* material whereas, in the case of our superlattice, it is the thickness of one of the constituent that is changing, modifying the *interfaces*. However, the disappearance of the rotations around the in-plane axis under tensile strain was also found in $LaNiO_3/SrMnO_3$ [15]. It is therefore another manifestation that, for small thicknesses, the interface effect

overrules the stress effect, and the effects in superlattices with a large number of interfaces are different than the ones in thin films with only one heterointerface.

As mentioned earlier, as the thickness of the $SrVO_3$ layer increases, the unit cell volume decreases and the rotations and tilts disappear. This is consistent with the general trend observed for $A^{3+}B^{3+}O_3$ perovskites under pressure, where rotations tend to disappear because AO_{12} dodecahedra are less rigid than BO_6 ones [25]. Such transitions under pressure lead from a low-symmetry phase to a high-symmetry phase, which is the case in our superlattice.

Regarding the resistive properties, the suppression of the octahedral rotations does not play a crucial role, as the overall temperature dependence stays the same for all superlattices. As $LaVO_3$ is an insulator [26] and $SrVO_3$ is metallic [27], the mobile charge carriers are likely to be located in the $SrVO_3$ layers of the superlattice. It was shown by studies of the band structure of $CaVO_3$ and $SrVO_3$ [28], that the V-O-V bond angle has no important effect on the electronic properties of the material. The bond angle of $CaVO_3$ is comparable to the bond angle observed for the $LaVO_3$ thin film [11], so at least for the 6/1 superlattice this may be a good estimation of the maximum possible change of bond angle in the $SrVO_3$ layer in the superlattices. As to $LaVO_3$, the influence of the octahedral rotations on the resistive properties was not studied until now to our knowledge. Theoretical studies show that the influence of strain and octahedral rotations may change the magnetic structure of $LaVO_3$ [29], but the size of the insulating gap is hardly influenced. So the absence of a fundamental change of the resistive properties in the superlattices without octahedral rotations compared to the 6/1 superlattice is not unexpected.

Going more into detail, an effect of the thickness of the $SrVO_3$ layers in the superlattice is seen on the temperature of the resistivity maximum: the temperature increases with increasing $SrVO_3$ thickness. Regarding the observed structural changes of the superlattices, at least two effects can be at the origin of this behavior: (i) the suppression of the octahedral rotations, and (ii) the reduction of the unit cell volume. It was shown that the evolution of the spin and orbital order temperatures in the rare-earth vanadates can be explained by considering the change in rare earth ionic size leading to different amplitudes of the octahedral rotation [30]. This theoretical treatment indicates that the transition temperature of the orbital order, which was shown to be related with the structural transition in $LaVO_3$ [22], increases with the amplitude of the octahedral rotation. As in the superlattices, the increase of the temperature of the resistive maximum is observed in samples with suppressed

rotations, this observation cannot be understood on the basis of this theory. Concerning the reduction of the unit cell volume, again the similarities of the resistive properties of all superlattices can be easily understood: the decrease of the unit cell volume leads to an enhanced overlap of the 3d vanadium orbitals and the 2p oxygen orbitals, favoring the conductivity of the $SrVO_3$ layers and the overall exchanges active in the superlattices. Thus, the enhanced temperature of the resistivity maximum could be a result of the enhanced orbital interaction in the $LaVO_3$ due to the reduced bond length. However, a multitude of other interaction channels of the structure and the resistivity are possible, and the origin of the resistivity maximum is still under investigation, so the above discussion is only a very rough sketch of the possible mechanisms in the superlattice.

V. CONCLUSION

The structure and the octahedral rotations were studied in $LaVO_3/SrVO_3$ superlattices with an increasing layer thickness of $SrVO_3$. Superlattices with a 1 unit cell thick $SrVO_3$ layer have an orthorhombic structure with a tilt pattern reminiscent of the bulk system, modified only by the epitaxial growth on a mismatched oxide. In superlattices with thicker $SrVO_3$, the octahedral rotations were suppressed, and the unit cell becomes metrically cubic with a reduced volume. These modifications cannot be explained by purely elastic effects due to the strain state of the superlattice, but the suppression of the octahedral tilts is favored by the presence of the rotation-free $SrVO_3$. The resistive properties of the superlattices are shown to be influenced only marginally.

Acknowledgements

The authors want to thank Hélène Rotella and Wilfrid Prellier for sample preparation, as well as Philippe Boullay and Raymond Frésard for intensive discussions. This research was partly supported by the ANR through the GeCoDo project (ANR-11-JS08-001-01), and the Conseil Régional de Basse Normandie, France in the framework of International Doctoral

School in Functional Materials (IDS FunMat).

---

[1] P. M. Woodward, Acta Crystallographica Section B **53**, 32 (1997).

[2] D. Viehland, Phys. Rev. B **52**, 778 (1995).

[3] Y. Noguchi, M. Miyayama, and T. Kudo, Phys. Rev. B **63**, 214102 (2001).

[4] L. Bellaiche and J. Íñiguez, Phys. Rev. B **88**, 014104 (2013).

[5] A. Y. Borisevich, H. J. Chang, M. Huijben, M. P. Oxley, S. Okamoto, M. K. Niranjan, J. D. Burton, E. Y. Tsymbal, Y. H. Chu, P. Yu, et al., Phys. Rev. Lett. **105**, 087204 (2010).

[6] P. Yu, J.-S. Lee, S. Okamoto, M. D. Rossell, M. Huijben, C.-H. Yang, Q. He, J. X. Zhang, S. Y. Yang, M. J. Lee, et al., Phys. Rev. Lett. **105**, 027201 (2010).

[7] H. T. Dang and A. J. Millis, Phys. Rev. B **87**, 155127 (2013).

[8] J. B. Goodenough, Progress in Solid State Chemistry **5**, 145 (1971).

[9] P. W. Anderson, Phys. Rev. **115**, 2 (1959).

[10] J. Kanamori, Journal of Physics and Chemistry of Solids **10**, 87 (1959).

[11] H. Rotella, U. Lüders, P.-E. Janolin, V. H. Dao, D. Chateigner, R. Feyerherm, E. Dudzik, and W. Prellier, Phys. Rev. B **85**, 184101 (2012).

[12] J. M. Rondinelli and N. A. Spaldin, Phys. Rev. B **82**, 113402 (2010).

[13] S. J. May, J.-W. Kim, J. M. Rondinelli, E. Karapetrova, N. A. Spaldin, A. Bhattacharya, and P. J. Ryan, Phys. Rev. B **82**, 014110 (2010).

[14] A. Vailionis, H. Boschker, W. Siemons, E. P. Houwman, D. H. A. Blank, G. Rijnders, and G. Koster, Phys. Rev. B **83**, 064101 (2011).

[15] S. J. May, C. R. Smith, J.-W. Kim, E. Karapetrova, A. Bhattacharya, and P. J. Ryan, Phys. Rev. B **83**, 153411 (2011).

[16] A. Glazer, Acta. Cryst. A **31**, 756 (1975).

[17] P. Bordet, C. Chaillout, M. Marezio, Q. Huang, A. Santoro, S.-W. Cheong, H. Takagi, C. Oglesby, and B. Batlogg, Journal of Solid State Chemistry **106**, 253 (1993).

[18] P. M. Woodward, Acta Crystallographica Section B **53**, 44 (1997).

[19] W. Sheets, P. Boullay, U. Lüders, B. Mercey, and W. Prellier, Thin Solid Films **517**, 5130 (2009).

[20] P. Boullay, A. David, W. C. Sheets, U. Lüders, W. Prellier, H. Tan, J. Verbeeck, G. Van Ten-

deloo, C. Gatel, G. Vincze, et al., Phys. Rev. B **83**, 125403 (2011).

[21] A. David, R. Frésard, P. Boullay, W. Prellier, U. Lüders, and P.-E. Janolin, Applied Physics Letters **98**, 212106 (2011).

[22] M. Rey, P. Dehaudt, J. Joubert, B. Lambert-Andron, M. Cyrot, and F. Cyrot-Lackmann, Journal of Solid State Chemistry **86**, 101 (1990).

[23] H. Y. Hwang, Y. Iwasa, M. Kawasaki, B. Keimer, N. Nagaosa, and Y. Tokura, Nature Mat. **11**, 103 (2012).

[24] A. J. Hatt and N. A. Spaldin, Phys. Rev. B **82**, 195402 (2010).

[25] R. J. Angel, J. Zhao, and N. L. Ross, Phys. Rev. Lett. **95**, 025503 (2005).

[26] S. Miyasaka, T. Okuda, and Y. Tokura, Phys. Rev. Lett. **85**, 5388 (2000).

[27] M. Onoda, H. Ohta, and H. Nagasawa, Solid State Communications **79**, 281 (1991).

[28] A. Sekiyama, H. Fujiwara, S. Imada, S. Suga, H. Eisaki, S. I. Uchida, K. Takegahara, H. Harima, Y. Saitoh, I. A. Nekrasov, et al., Phys. Rev. Lett. **93**, 156402 (2004).

[29] H. Weng and K. Terakura, Phys. Rev. B **82**, 115105 (2010).

[30] P. Horsch, A. M. Oleś, L. F. Feiner, and G. Khaliullin, Phys. Rev. Lett. **100**, 167205 (2008).